Journal of Physical Science, Vol. 33(3), 1–15, 2022

Effect of Coupling Agent on Properties of Composites Made from Styrofoam Waste and Coconut Shell

Koay Seong Chun,[1*] Subhramani Thangamuthu,[2] Chan Ming Yeng[3] and Ong Thai Kiat[4]

[1]Department of Mechanical and Materials Engineering, Lee Kong Chian Faculty of Engineering and Science, Universiti Tunku Abdul Rahman, Jalan Sungai Long, Bandar Sungai Long, Cheras 43300, Kajang, Selangor, Malaysia
[2]School of Engineering, Faculty of Innovation and Technology, Taylor's University Lakeside Campus, No. 1, Jalan Taylor's, 47500 Subang Jaya, Selangor, Malaysia
[3]Department of Materials Engineering, Tunku Abdul Rahman University College, Kampus Utama, Jalan Genting Kelang, 53300 Kuala Lumpur, Malaysia

[*]Corresponding author: koaysc@utar.edy.my

Published online: 30 November 2022

To cite this article: Koay, S. C. et al. (2022). Effect of coupling agent on properties of composites made from styrofoam waste and coconut shell. *J. Phys. Sci*., 33(3), 1–15. https://doi.org/10.21315/jps2022.33.3.1

To link to this article: https://doi.org/10.21315/jps2022.33.3.1

ABSTRACT: *Styrofoam is amongst one of the highly used packaging materials due to its lightweight and vibration isolate properties. The usage of styrofoam rises yearly, but it is seldom received by the recycling facilities to recycle the post-consumed styrofoam due to the poor economic viability. The objective of this research is to investigate the potential value of recycling post-consumed styrofoam as feedstock in producing sustainable composite materials. Therefore, this study would increase the feasibility and interest in recycling of styrofoam and indirectly continue the life cycle of styrofoam waste. In this study, the composites with varying compositions were of recycled polystyrene (rPS), coconut shell (CS) and maleated polystyrene (MAPS) compounded using an internal mixer. The effects of compositions on torque rheological, flexural and morphological properties of the composites were investigated. The findings showed that rPS/CS composites filled with more CS content possesses higher processing torque due to increase in viscosity. However, addition of MAPS lowered the viscosity of composites. The flexural properties revealed that the rPS/CS composites without MAPS exhibited the highest flexural strength and modulus of 33.5 MPa and 3.1 GPa, respectively, when the CS content was measured at 30 wt%. Then, the addition of MAPS improved on average 29% of flexural strength and 14% of flexural modulus, individually. The results from scanning electron microscopy showed that the addition of MAPS had improved the interfacial adhesion between rPS matrix and CS particles, which resulted in an improvement on flexural properties. The*

flexural properties of rPS/CS composites are comparable to wood plastic composites (WPC) as found in literature, which demonstrates its potential to be used in applications similar to WPC.

Keywords: styrofoam waste, coconut shell, composites, coupling agent

1. INTRODUCTION

In the early 1990s, composites made from wood fibre and thermoplastic or thermoset, also called as wood plastic composite (WPC) were first widely marketed.[1] These composites were being used as decking material because it exhibited a better weather resistance than the natural wood. Soon, these composites were developed into other applications, such as fencing, furniture and automotive parts. Initially, saw dust or fine wood flour were compounded with thermoplastic, such as polyethylene and polypropylene for producing WPC.[2] The adding of wood fibre to thermoplastic lowered WPC cost, enhanced the stiffness and reduced the coefficient of thermal expansion.[3] Recently, WPC has been produced using recycled plastic and agricultural wastes, such as coconut shell (CS),[4,5] rice husk[6] and oil palm's empty fruit bunch,[7] which provide benefits, such as it reduces the product footprint in environment, increases the utilisation rate of agricultural waste and increases recycling rate of plastic wastes. The IKEA ODGER chair is a good example of a WPC application that is made from reclaimed wood waste and recycled plastic.[8]

Coconut is an important crop widely grown in tropical countries, such as India, Indonesia, Malaysia, Thailand, Sri Lanka, Philippine and Brazil.[9] In food and beverage industry, coconut juice is packaged as ready-to-drink beverage. Furthermore, coconut milk and coconut oil can be extracted from coconut flesh. The coconut husk and shells are non-edible parts of the coconut, which is generally disposed of as waste from the industry. In Malaysia, there are industries that collect CS and resell them in powder form. The CS powder is frequently used as biofuel and produces activated carbon.[4] In recent years, scientific research has reported the potential of utilising CS as an alternative filler for producing composites. Previous studies related to CS filled thermoplastic composites have shown that the addition of CS has increased the stiffness and thermal stability of the composites.[4,5,9] The present study aims to further explore the potential of incorporating CS as filler in producing composite materials.

Styrofoam is commercially named as closed cell extruded polystyrene (PS) foam, also called expanded PS. The styrofoam contains more than 95% of air in the composition, and this makes it an exceptional thermal insulator and shock

absorbent which is that ideal for packaging applications.[8,10] The recycling of styrofoam wastes has a logistical challenge in compacting the storage due to its lightweight composition. The logistical expenses of styrofoam wastes are relatively expensive, and the resale value of recycled PS resin made from styrofoam wastes is much more expensive than new PS resin. This makes the recycling of styrofoam financially irrational. For this reason, majority of styrofoam waste is deposited into landfills and causes environmental pollution. Furthermore, the styrofoam waste often ends up in the waterways that result them to turn into a pollutant for wild animals.[11] Thereupon, this research aims to investigate the potential of recycling styrofoam wastes and converting them into composite material that can be used as WPC. The selling price of WPC is significantly higher than raw PS resin and turning the styrofoam wastes into WPC is financially feasible.

The main challenge in producing WPC is difficulty in obtaining a homogenous filler dispersion and great filler-matrix adhesion. Natural filler naturally has a more hydrophilic character because it contains more hydroxyl functional groups in chemical structure. The polarity difference between natural filler and polymer matrix causes poor interfacial adhesion.[12] To overcome the challenge, the maleated co-polymer is often used to enhance the interfacial adhesion between natural filler and polymer matrix. Meleated co-polymer is a polymer grafted with maleic anhydride groups. These maleic anhydride groups are highly reactive towards the hydroxyl group of natural filler during the compounding process. The coupling effect from the maleated co-polymer is contributed by chemical bonding formed between natural filler and the maleic anhydride side group. Meanwhile, the polymer chains from the co-polymer are chemically bonded to the natural filler and provides a high degree of entanglement with polymer chains from the matrix.[13] This reaction significantly enhances the adhesion between natural filler and polymer matrix. The study from literature found that the addition of maleated polystyrene (MAPS) with the presence of processing aid significantly increase both the tensile strength and modulus of recycled polystyrene (rPS)/CS composites.[4] Nevertheless, there is no literature that has considered investigating the effect of filler content and MAPS on torque rheological and flexural properties of rPS/CS composites. A feat is implemented in this study towards property enhancement of rPS/CS composites.

It was reported from previous works that the study on rPS/CS composites just focused on tensile, thermal and morphological properties.[4] For current research, the effects of filler content and MAPS on torque rheological, flexural and morphological properties of rPS/CS composites are reported.

2. METHODOLOGY

2.1 Materials

The CS powder with average particle size of 149 microns was supplied by Sekimdi Industries Sdn. Bhd. (Sabak Bernam, Selangor, Malaysia). The styrofoam wastes were retrieved from local electrical appliance retailers around Subang Jaya district in Malaysia. The MAPS were used as a coupling agent and was obtained from Sigma Aldrich Malaysia (Selangor, Malaysia).

2.2 Preparation of Recycled Polystyrene

The collected styrofoam wastes were first cut into smaller pieces with size not larger than 4 cm. Then, the styrofoam pieces were transferred into an air circulated oven (brand Memmert, Schwabach, Germany) at 140°C for 15 min. Then, the styrofoam pieces were shrunk into hard and rigid rPS crumbs. This released entrapped air from the foam and was left with PS resin. The rPS crumbs were kept in a sealed plastic bag.

2.3 Preparation of Composites

The rPS crumbs and CS powder were compounded using Brabender® Plastograph internal mixer Model EC PLUS (Duisburg, Germany) at a temperature maintained at 190°C and rotor speed of 80 rpm. The composites were formulated with rPS/CS in a ratio of 70:30, 55:45 and 40:60. A similar method was also used for compounding the rPS/CS composites with MAPS, but 3 wt% of MAPS resin was added together with rPS crumbs. The sequences of compounding were: (i) transfer the rPS crumbs into mixing chamber and wait for the rPS to melt within 2 min; (ii) after 2 min, add CS powder into melted rPS; (iii) continuous compound for 8 min and (iv) last, remove the mixture from the mixing chamber.

Then, the rPS/CS mixture was moulded into a sheet having a dimension of 150 mm x 15 mm and 3 mm of thickness. The compression moulding machine used in this experiment was the Gotech Model: GT 7014A (Taichung, Taiwan) and temperature fixed at 190°C. The sequences of compression moulding were: (i) preheat the mixture for 4 min; (ii) fully compress the sample at 1 ton of force for 1 min and (iii) place the sample under a cooling plate until the temperature reduced to room temperature. The flexural specimens were cut from rPS/CS composites sheets using bandsaw with the dimension in accordance to ASTM D790.

2.4 Testing and Analysis

The torque rheological properties of the rPS and CS composites with and without MAPS were obtained using Brabender® Plastograph internal mixer Model EC PLUS with counter-rotating rotor (Duisburg, Germany). The analysis method was referred to the method reported by Chun et al.[13,14] The temperature of the mixing chamber was maintained at 190°C and the rotor speed was controlled at 40 rpm, 60 rpm and 80 rpm. This equipment recorded the processing torque along the test time by the Brabender® Mixer Program (WINMIX). The processing characteristics of the mixture were displayed as processing torque versus time. The processing torque at end time M versus rotor speed S was plotted on a log scale according to Equation 1.[15,16]

$$M = CS^b \tag{1}$$

Where C is a constant that depends on the geometry of the equipment and b is another constant for flow behaviour of melted polymer melt. The gradient of log M versus log S graph is calculated as constant b. The constant b is considered equivalent to the melt flow index n for non-Newtonian fluids that obey the power law model in Equation 2.[15,16]

$$\tau = K\gamma^n \tag{2}$$

Where τ is shear stress, K is a constant for flow consistency and γ is the shear rate. The τ and γ of the melted polymer can be calculated from the measured processing torque and rotor speed using Equations (3) and (4), respectively. Both equations are modified for non-Newtonian fluids that are measured using the Brabender® Plastograph internal mixer. The viscosity η can be calculated using Equation (5) .[15,16]

$$\tau_1 = \frac{M_1}{2\pi R_m^2 h} \tag{3}$$

$$\gamma_1 = \frac{2S1}{nR_m^{2/n}\left(R_i^{-2/n} - R_e^{-2/n}\right)} \tag{4}$$

$$\eta = \frac{\tau_1}{\gamma_1} \tag{5}$$

The effective instrument dimensions of the Brabender® Plastograph internal mixer Model EC PLUS are inner radius diameter, Ri = 1.65 cm, outer radius diameter, Re = 1.85 cm, average radius diameter, Rm = 1.75 cm and cylinder length, h = 4.6 cm.

The rPS/CS composites were tested for its flexural properties using Instron universal testing machine (model 5596, Norwood, Massachusetts, USA) in accordance with ASTM D790 standard. A load cell with capacity of 15 kN was used, and crosshead speed was set at 5 mm/min. A minimum of 7 specimens were tested for each formulation. The data collected from the flexural test were analysed using Microsoft Excel 365 enterprise with ANOVA single factor analysis. The difference between the test results of the specimens were considered significant when p value ≤ 0.05.

The fracture specimens of rPS/CS composites of selected composition were analysed and examined using field emission scanning electron microscope (FESEM) equipment, Bruker Mini SEM model: SNE-3000M. The specimens were sputter coated with an ultra-thin layer of gold to prevent charges during the observation. The acceleration voltage of the equipment was set at 30 keV.

3. RESULT AND DISCUSSION

3.1 Torque Rheological Properties

Figure 1 shows the plot of processing torque against time for neat rPS, rPS/CS composites with and without MAPS at 40 rpm and 190°C. A sharp peak at the first minute was observed when the rPS crumbs transferred into the mixing chamber. The presence of solid and rigid rPS crumbs restricted the motion of the moving rotor, causing the increase in processing torque. Once the rPS crumbs began to melt, the processing torque reduced gradually and maintained at a relatively constant torque value, as observed in neat rPS. The processing torque before 2 min was getting lower as the filler content increased. This observation was due to deduction of rPS content, which reduced the amount of torque required to shear the rPS crumbs. For rPS/CS composites, a second process torque developed after 2 min. This is because the addition of CS powder interrupted the melt flow of the melted rPS. The second peak of processing torque increased when added with more filler content. For rPS/CS composites, the process torque was slowly decreased and became stable at constant torque until the end of compounding time. The mixing characteristic of rPS/CS composites using Brabender® Plastograph internal mixer was similar to composites with different natural fillers.[5,13,14]

The stabilised torque at compounding end time was obtained from the plot of processing torque against time at different rotor speed. The obtained data was plotted into log torque versus log rotor speed as displayed in Figure 2. The measured processing torque was increased as the rotor speed increased. As melted compound increased, rotor speed increased due to the magnitude of the friction and constraints.[17] The processing torque of rPS/CS composites increased when

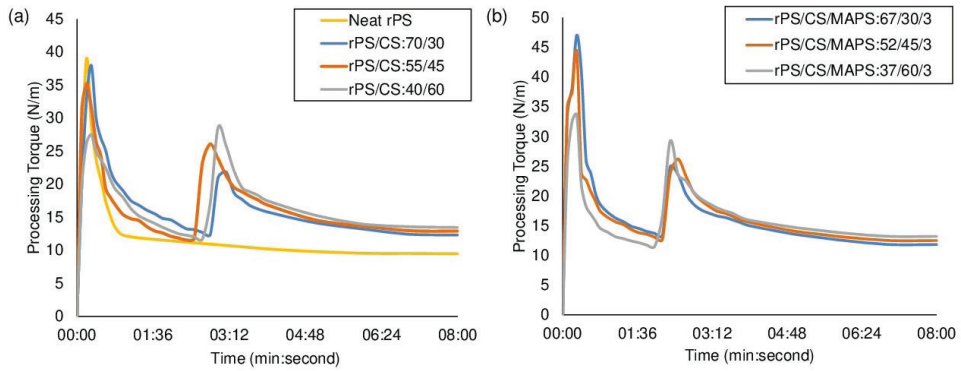

Figure 1: (a) Plot of processing torque against time for neat rPS, rPS/CS composites with MAPS at 40 rpm and 190ºC and (b) Plot of processing torque against time for neat rPS, rPS/CS composites without MAPS at 40 rpm and 190ºC.

the filler content was compared to neat rPS. The addition of fine solid particles of CS hindered the flow of the melted rPS and this effect was increased after adding more filler. Therefore, a higher torque was required to overcome the melt flow restriction caused by the filler to disperse the filler into a homogenous mixture. Observably, the increase in filler content directly increased the viscosity of the rPS/CS compound. A similar observation was also reported by Chun et al.[13,14] in compounding of polypropylene/cocoa pod husk composites. The addition of MAPS significantly reduced the processing torque of rPS/CS composites. The maleated co-polymer is usually a lower molecular weight polymer compared to the polymer matrix. Therefore, addition of maleated co-polymer exhibited an external lubricating effect on composite materials during the melt compounding process.[18] The presence of MAPS also showed a lubricating effect that reduced the processing torque and viscosity of rPS/CS compounding. Adhikary et al.[19] also discovered that the addition of maleated polyethylene benefits the compounding of high-density polyethylene/wood fibre composites by lowering the viscosity due to its lubricating effect. From Figure 2, the slope of the plot can be obtained as melt flow index *n*. The value *n* for neat rPS and both rPS/CS composites were lower than 1. These materials depict pseudoplastic behaviour. As the filler content increased, the value *n* of rPS/CS composites got smaller. This indicated that rPS/CS composites with more filler content show more shear thinning effect at higher shear rate. Moreover, the value *n* of rPS/CS composites with MAPS were slightly lower than rPS/CS composites without MAPS. The addition of MAPS reduced the pseudoplasticity of rPS/CS composites.

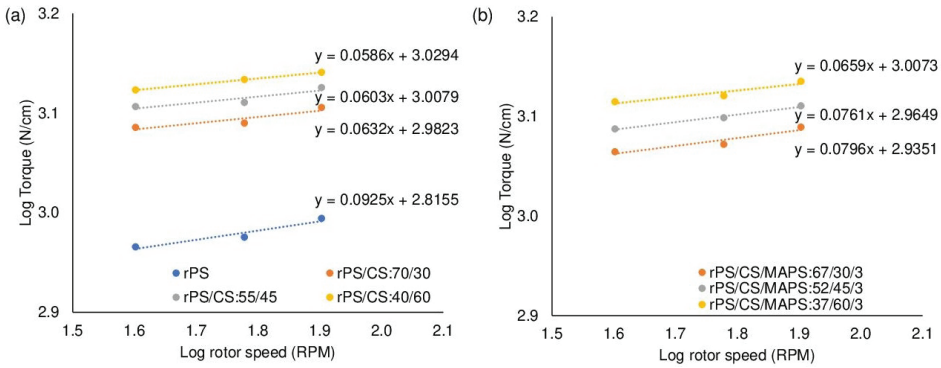

Figure 2: (a) Plot of log torque against log rotor speed of neat rPS, rPS/CS composites with MAPS and (b) Plot of log torque against log rotor speed of neat rPS, rPS/CS composites without MAPS.

Figure 3 displays the relationship between shear stress and shear rate of the melted neat rPS and rPS/CS composites with and without MAPS. The shear stress of the melted compound was increased with the increase in shear rate. As mentioned earlier, the viscosity of the rPS/CS composites was highly influenced by the filler content. Consequently, the equipment needed higher shear stress to generate more shearing action in the melted compound to overcome the restriction of melted polymer formed caused by the filler. Alternatively, the addition of MAPS benefits in compounding the rPS/CS composites, as the overall shear stress was lower than rPS/CS composites without MAPS. The decrease in the shear stress of rPS/CS composites was due to the lubricating effect from MAPS.

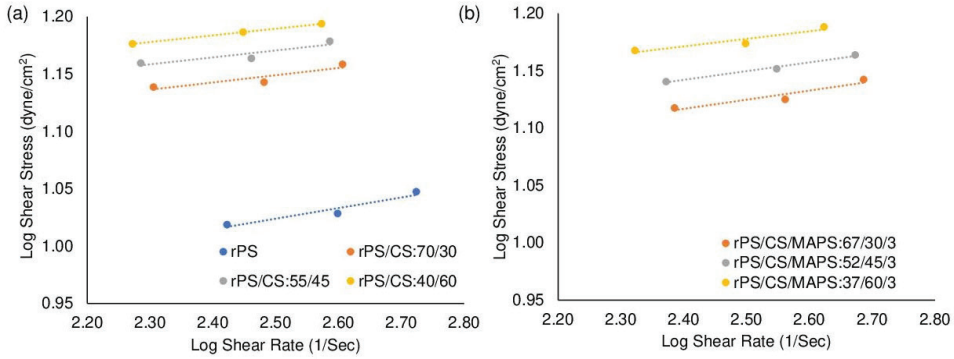

Figure 3: (a) Plot of log shear stress against log shear rate of neat rPS, rPS/CS composites with MAPS and (b) Plot of log shear stress against log shear rate of neat rPS, rPS/CS composites without MAPS.

Figure 4 shows the plot of viscosity versus shear rate of neat rPS and rPS/CS composites with and without MAPS. The increased shear rate significantly reduced the viscosity of neat rPS and both rPS/CS composites. The chain entanglement from rPS matrix reduces at a higher shear rate, and this is called the shear thinning effect. Other researchers also agreed that the increase in shear rate causes a shear thinning effect in natural filler filled thermoplastic composite materials.[13,14] However, from Figure 4, the viscosity of rPS/CS composites significantly increased with addition of more filler content. This is because, the addition of CS powder hindered the melting flow of the compound as the CS particles tend to agglomerate, especially when composite added with higher filler content. However, the presence of MAPS was chemically attached on the CS particles, and avoid CS particles from agglomeration; thus this might further improve the filler dispersion and increase the melting flow of compound. Also, the presence of MAPS introduced a lubricating effect of the rPS/CS composites during the compounding, the viscosity of the melted rPS/CS compound with MAPS was lower than rPS/CS compound without MAPS. The reduction of melt viscosity is beneficial for compounding a composite material with high filler content because the process might consume less energy. Researchers also noticed that the addition of maleated co-polymer on composites containing natural filler exhibited lower viscosity during the compounding.[18,19]

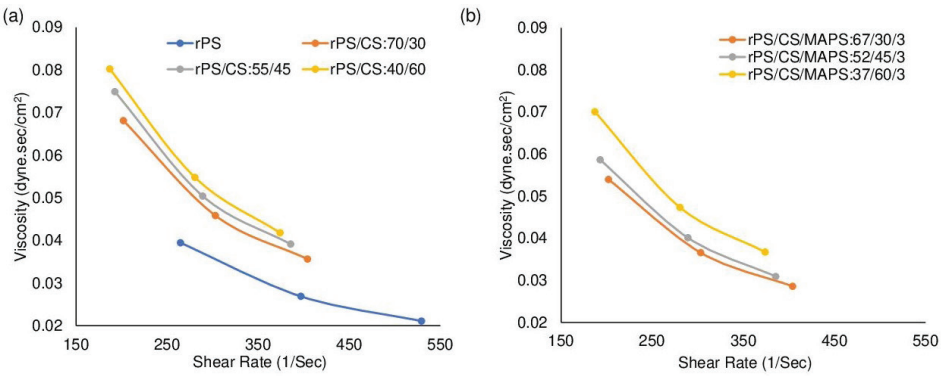

Figure 4: (a) Plot of viscosity against shear rate of neat rPS, rPS/CS composites with MAPS and (b) Plot of viscosity against shear rate of neat rPS, rPS/CS composites without MAPS.

3.2 Flexural Properties

Flexural test is usually known as testing the ability of a composite material to bend. Flexural tests include different types of load conditions, such as compression load

on the top surface, shear load at the central portion and tensile load at bottom face.[20] The flexural strength and modulus of neat rPS and rPS/CS composites with and without MAPS of different filler content are depicted in Figure 5. As compared to neat rPS, the addition of 30 wt% of filler content increased the flexural strength and modulus of rPS/CS composites, without MAPS by 8.8% and 30%, respectively. However, the flexural strength and modulus of rPS/CS composites gradually decreased when the filler content exceeded 30 wt%. At a filler content of 30 wt%, the composite has a correct proportion of rPS matrix that can wet the majority of the CS particles and form a good adhesion with the CS. Once the filler content exceeds 30 wt%, the matrix becomes less and difficult to form a good adhesion with the CS particles, and this decreases the flexural properties of the composites. The composite material usually has a threshold point for the filler content to achieve the optimum mechanical properties. If beyond the threshold point, the composite usually shows weaker mechanical properties.[21]

Regarding Figure 5, the rPS/CS composites with MAPS showed on average 29% higher flexural strength and 14% higher flexural modulus as compared to rPS/CS composites without MAPS. As shown in Figure 6, the presence of MAPS were chemically bonded on the CS particle's surface via maleic anhydride groups grafted on the MAPS. Therefore, the PS chains from the MAPS were indirectly bonded on the CS particles' surface and entangled with the rPS chains of the matrix. As a result, the rPS matrix was able to form a better adhesion with the CS particles. The presence of MAPS significantly enhanced the flexural properties of rPS/CS composites. As reported by Hyvarinen et al.,[22] the WPC from polypropylene and 64 wt% of wood fibre exhibited a flexural strength of 23 MPa and flexural modulus of 4.44 GPa. In addition, Pao and Yeng[23] also found that WPC made from expanded polystyrene and alkaline treated coconut shell powder at filler content of 65 wt% via solvent casting method, was able to obtain flexural strength and modules of 18 MPa and 3.3 GPa, respectively. In comparison, the flexural properties of rPS/CS composites with MAPS are comparable with WPC found in literature.

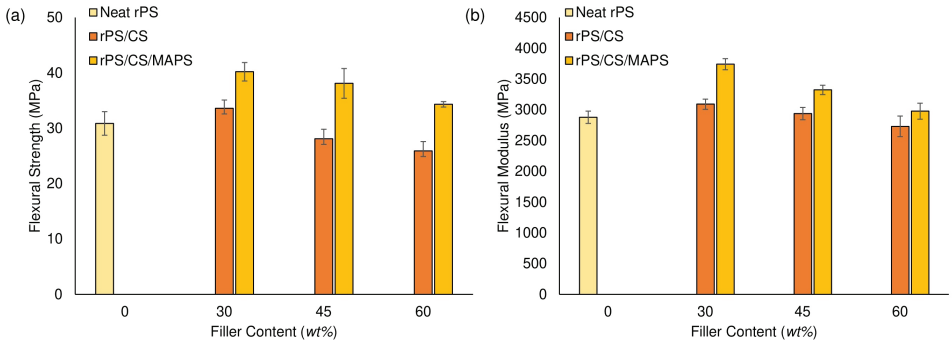

Figure 5: (a) Flexural strength and (b) flexural modulus of neat rPS, rPS/CS composites with and without MAPS.

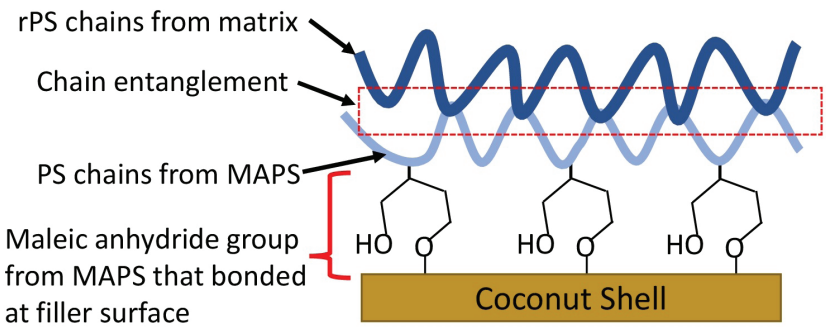

Figure 6: Schematic reaction when rPS/CS composites added with MAPS.

3.3 Morphological Properties

The SEM micrograph taken at CS particles is displayed in Figure 7(a). The CS particles were in irregular shape and low aspect ratio. Figure 7(b) shows the SEM micrograph of the fracture surface of the neat rPS matrix. The SEM micrograph of neat rPS displayed a brittle fracture surface with a homogenous matrix tearing. This indicated that rPS has brittle fracture behaviour. Figure 8 depicts SEM micrograph of rPS/CS composites without MAPS at selected filler content. According to Figure 8(a), the CS particles were embedded in rPS matrix when the filler content was at 30 wt%. This indicated that the rPS was able to wet majority of the CS particles to form a good adhesion when the filler content was at 30 wt%. For this reason, the rPS/CS composites with 30 wt% exhibited the highest value of flexural strength and modules. From Figure 8(b), several holes caused by filler pull out were observed in rPS/CS composites without MAPS at 60 wt% of filler

content. It was evident that the adhesion between CS particles and rPS matrix was getting worse, as the amount of rPS matrix became lesser and unable to wet most of the CS particles. This finding supported the reason why flexural strength and modulus of rPS/CS composites with 30 wt% of filler content was highest, but the flexural strength and modulus of composites reduced as the filler content increased up to 60 wt%. The SEM micrographs of fracture surface of rPS/CS composites with MAPS at selected filler content are shown in Figure 9. The CS particles were found well coated and remain embedded in rPS matrix after being fractured. The observation from SEM micrographs proved that addition of MAPS established a better adhesion between CS particles and rPS matrix, which proven the addition of MAPS was able to increase the flexural strength and modulus of rPS/CS composites discussed in an earlier section of this article.

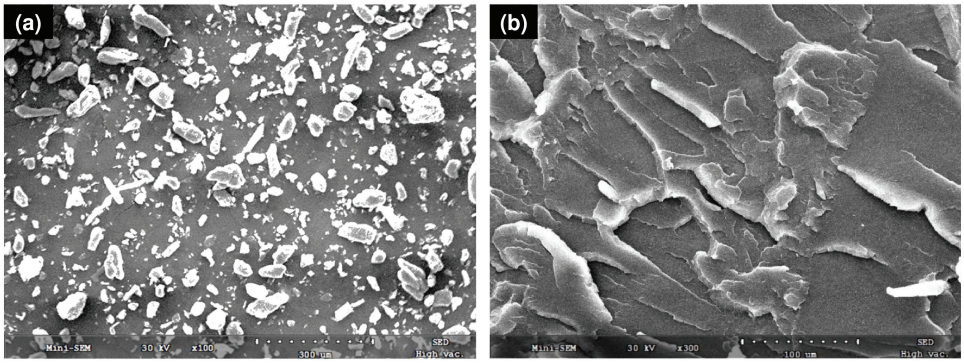

Figure 7: (a) SEM Micrographs of CS particles and (b) SEM Micrographs fracture specimen of neat rPS.

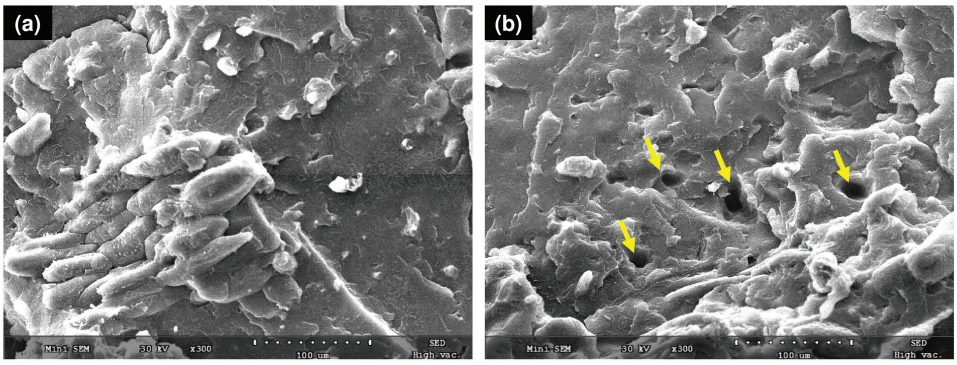

Figure 8: (a) SEM Micrographs of rPS/CS composites without MAPS at 30 phr filler content and (b) SEM Micrographs of rPS/CS composites without MAPS at 60 phr of filler content.

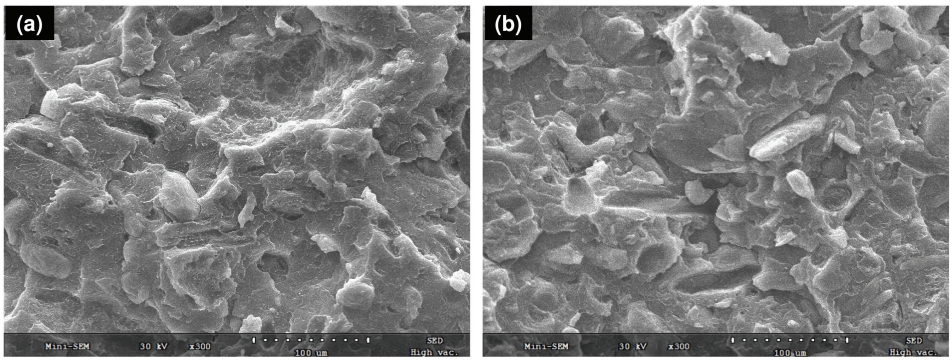

Figure 9: (a) SEM Micrographs of rPS/CS composites with MAPS at 30 phr of filler content and (b) SEM Micrographs of rPS/CS composites with MAPS at 60 phr of filler content.

4. CONCLUSION

The melted neat rPS and rPS/CS composites with and without MAPS exhibited a pseudoplastic behaviour during the melt compounding, and it underwent shear thinning at higher shear rate. The processing torque of the rPS/CS composites increased with the increase in filler content due to the change in viscosity. However, the addition of MAPS significantly reduced the processing torque of the rPS/CS composites due to reduction of melt viscosity caused by lubricating effect from MAPS. This indicated that the addition of MAPS benefits in lowering the shear stress when compounding the rPS/CS composites at high amounts of filler content. Both rPS/CS composites achieved optimum flexural strength and modulus when filler content was at 30 wt%. Once the filler content exceeded 35 wt%, the flexural strength and modulus of these composites reduced. Alternatively, the rPS/CS composites with MAPS exhibited an average of 29% and 14% individually higher flexural strength and flexural modulus compared to rPS/CS composites without MAPS. This proved that the presence of MAPS enhanced the interfacial adhesion between CS particles and rPS matrix, which led to an improvement in flexural properties. The SEM micrograph also showed that there was a sufficient adhesion between particles and rPS matrix at filler content of 30 wt% and the addition of MAPS. In short, the rPS/CS composites demonstrated comparable properties compared to WPC, and it is potentially efficient to be used in applications similar to WPC.

5. ACKNOWLEDGEMENT

The authors gratefully acknowledge use of services and facilities at Taylor's University and Tunku Abdul Rahman College University.

6. REFERENCES

1. Md Zahaidul, I. et al. (2022). Green composites from natural fibers and biopolymers: A review on processing, properties, and applications. *J. Reinf. Plast. Compos.*, 41(13–14), 526–557. https://doi.org/10.1177/07316844211058708
2. Keskisaari, A., & Karki, T. (2018). The use of waste materials in wood-plastic composites and their impact on the profitability of the product. *Resour. Conserv. Recycl.*, 134, 257–261. https://doi.org/10.1016/j.resconrec.2018.03.023
3. Satya, G. N. et al. (2022). Development of wood polymer composites from recycled wood and plastic waste: Thermal and mechanical properties. *J. Compos. Sci.*, 6(7), 194–207. https://doi.org/10.3390/jcs6070194
4. Ling, S. L. et al. (2020). Wood plastic composites produced from postconsumer recycled polystyrene and coconut shell: Effect of coupling agent and processing aid on tensile, thermal, and morphological properties. *Polym. Eng. Sci.*, 60(1), 202–210. https://doi.org/10.1002/pen.25273
5. Chun, K. S. et al. (2013). Characterization and properties of recycled polypropylene/coconut shell powder composites: Effect of sodium dodecyl sulfate modification. *Polym. Plast. Technol. Eng.*, 52(3), 287–294. https://doi.org/10.1080/03602559.2012.749282
6. Chen, R. S. et al. (2016). Characterization of rice husk-incorporated recycled thermoplastic blend composites. *Bioresour.*, 11(4), 8470–8482. https://doi.org/10.15376/biores.11.4.8470-8482
7. Tan, C. et al. (2011). Characterization of polyester composites from recycled polyethylene terephthalate reinforced with empty fruit bunch fibers. *Mater. Des.*, 32(8–9), 4493–4501. https://doi.org/10.1016/j.matdes.2011.03.037
8. Chun, K. S. et al. (2018). Wood plastic composites made from corn husk fiber and recycled polystyrene foam. *J. Eng. Sci. Technol.*, 13(11), 3445–3456.
9. Chun, K. S. et al. (2013). Properties of coconut shell powder-filled polylactic acid ecocomposites: Effect of maleic acid. *Polym. Eng. Sci.*, 53(5), 1109–1116. https://doi.org/10.1002/pen.23359
10. Koay, S. C. et al. (2019). Wood plastic composites made from post-used polystyrene foam and agricultural waste. *J. Thermoplast. Compos. Mater.*, 32(11), 1455–1466. https://doi.org/10.1177/0892705718799836
11. Jang, M. et al. (2016). Styrofoam debris as a source of hazardous additives for marine organisms. *Environ. Sci. Technol.*, 50(10), 4951–4960. https://doi.org/10.1021/acs.est.5b05485
12. Marathe, D. et al. (2022). Study of effect of wood-flour content on mechanical, thermal, rheological properties and thermoformability of wood-polypropylene composites. *J. Polym. Eng.*, 42(1), 1–8. https://doi.org/10.1515/polyeng-2021-0153

13. Chun, K. S. et al. (2019). Torque rheological properties of polypropylene/cocoa pod husk composites. *J. Thermoplast. Compos. Mater.*, 30(9), 1217–1227. https://doi.org/10.1177/0892705715618743
14. Chun, K. S. et al. (2018). Torque rheological properties of agro-waste-based polypropylene composites: Effect of filler content and green coupling agent. *J. Vinyl. Addit. Technol.*, 24(S1), E30–E35. https://doi.org/10.1002/vnl.21561
15. Babbar, I., & Mathur, G. N. (1994). Rheological properties of blends of polycarbonate with poly(acrylonitrile-butadiene-styrene). *Polym.*, 35(12), 2631–2635. https://doi.org/10.1016/0032-3861(94)90391-3
16. Goodrish, J. E., & Porter, R. S. (1967). A rheological interpretation of torque-rheometer data. *Polym. Eng. Sci.*, 7(1), 45–51. https://doi.org/10.1002/pen.760070112
17. Rahman, W. A. et al. (2010). Rice Husk/High Density Polyethylene Bio-Composite: Effect of Rice Husk Filler Size and Composition on injection molding processability with respect to impact property. *Adv. Mater. Res.*, 83–86, 367–374. https://doi.org/10.4028/www.scientific.net/AMR.83-86.367
18. Luan, L. et al. (2011). Rheological behavior of lubricating systems in polypropylene/seaweed composites. *J. Appl. Polym. Sci.*, 121(4), 2143–2148. https://doi.org/10.1002/app.33940
19. Adhikary, K. B. et al. (2011). Effects of lubricant content on extrusion processing and mechanical properties of wood flour-high-density polyethylene composites. *J. Thermoplast. Compos. Mater.*, 24(2), 155–171. https://doi.org/10.1177/0892705710388590
20. Mirmehdi, S. M. et al. (2014). Date palm wood flour as filler of linear low-density polyethylene. *Compos. Part B Eng.*, 56, 137–141. https://doi.org/10.1016/j.compositesb.2013.08.008
21. Fiore, V. et al. (2018). Experimental design of the bearing performances of flax fiber reinforced epoxy composites by a failure map. *Compos. Part B Eng.*, 148, 40–48. https://doi.org/10.1016/j.compositesb.2018.04.044
22. Hyvarinen, M. et al. (2019). The effect of the use of construction and demolition waste on the mechanical and moisture properties of a wood-plastic composite. *Compos. Struct.*, 210, 321–326. https://doi.org/10.1016/j.compstruct.2018.11.063
23. Pao, C. Z., & Yeng, C. M. (2019). Properties and characterization of wood plastic composites made from agro-waste materials and post-used expanded polyester foam. *J. Thermoplast. Compos. Mater.*, 32(7), 951–966. https://doi.org/10.1177/0892705718772877